Thin-Walled Structures 132 (2018) 120–135

Contents lists available at ScienceDirect

Thin-Walled Structures

journal homepage: www.elsevier.com/locate/tws

Full length article

Simulation of fracture of a tubular X-joint using a shear-modified Gurson–Tvergaard–Needleman model

Jintai Liu[a], Shen Yan[a,b], Xianzhong Zhao[a,c,*]

[a] College of Civil Engineering, Tongji University, Shanghai 200092, China
[b] School of Civil Engineering, The University of Sydney, Sydney, NSW 2006, Australia
[c] State Key Laboratory of Disaster Reduction in Civil Engineering, Shanghai 200092, China

ARTICLE INFO

Keywords:
Joint test
Square hollow section (SHS) X-joint
Ductile fracture
Fracture model
Coupon test

ABSTRACT

The full-range behaviour of materials and connections is important in the research of progressive collapse resisting mechanisms and structural seismic behaviour. There have been several recent studies on the fracture simulation of tubular joints. However, the reliability of the fracture models adopted for the tubular members, as well as for the weld materials, has not been examined under various stress states. This paper firstly describes an experimental study on square hollow section X-joint under axial loading. The joint is well tested into the post-ultimate range, and fracture occurs through the thickness of the chord. For the tubular sections and welds used in the joint, three types of coupon tests are carried out for each material, based on which a standard procedure for calibrating the parameters of the Gurson–Tvergaard–Needleman (GTN) model is proposed. Finite-element simulations of the joint test using the calibrated GTN model are then performed. The results show that the original GTN model can predict the initiation of cracks in the X-joint, but fails to predict the fracture propagation, under a shear-dominated stress state, with sufficient accuracy. A shear-modified GTN (referred to as SMGTN) model is developed by combining the GTN model with a maximum shear stress criterion, and shows better performance than the original GTN model, according to the simulated results, in predicting the entire fracture process.

1. Introduction

Tubular joints have excellent mechanical properties, good appearance, and economic rust-proof processing, and thus are commonly used in high-rise buildings, large-span roofs, and bridges. Substantial research has been carried out with the aim of determining the stiffness and bearing capacity of a variety of tubular joints [1–3]. However, considerably fewer investigations have examined the post-ultimate behaviour and the subsequent material fracture, which marks the total failure of the tubular joint. The full-range behaviour, from the elastic response to the fracture of joint components, is important for progressive collapse analysis and for seismic applications in which the energy absorbed by the structure is to be calculated over the full range of the joint response. Therefore, more attention should be paid to the post-ultimate behaviour of tubular joints, especially to fractures occurring either in tubular members or in welds.

Makino and Kurobane [4] introduced a database consisting of 1516 test results and 782 finite-element (FE) analysis results for unstiffened T, X, K, TT, XX, TX, and KK circular hollow section (CHS) tubular joints. This database was created to evaluate existing design formulas and facilitate new ultimate capacity equations. However, few of these experimental and FE investigations were performed into the fracture and post-fracture range, and thus cannot provide experimental evidence for fracture simulations of tubular joints.

There have been several recent studies on the fracture simulation of tubular joints. Using a model based on the Continuum Damage Mechanics (CDM), Cofer et al. [5] performed FE simulations to study the fracture behaviour of a T-joint and a DT-joint. Further applications of the CDM models in fracture simulation of T-, K-, and KK-joints were considered by Wang et al. [6]. Ma et al. [7] adopted a modified CDM-based model to simulate the fracture of tubular X-joints with CHS branches to a square hollow section (SHS) chord, a structure that was tested by Wang et al. [8]. Tousignant and Packer [9,10] investigated the capacity of fillet welds in CHS X-joints through tests and FE parametric analyses using a constant critical strain criterion. Fei et al. [11,12] utilised the extended Mohr–Coulomb ductile fracture criterion [13] to simulate punching shear fractures in longitudinal plates to concrete-filled CHS connections. Qian et al. [14] employed the extended Gurson model [15–17] to simulate fractures in pre-cracked X-joints and intact X-/K-joints.

* Corresponding author at: College of Civil Engineering, Tongji University, Shanghai 200092, China.
E-mail address: x.zhao@tongji.edu.cn (X. Zhao).

https://doi.org/10.1016/j.tws.2018.07.054
Received 13 May 2018; Received in revised form 15 July 2018; Accepted 30 July 2018
0263-8231/

Nomenclature

C_1, C_2	parameters proposed in a logarithmic true stress–logarithmic strain law
D	scalar damage variable
T	stress triaxiality
b_0	initial width of a tensile plate
b_f	width of the fracture surface of a tensile plate
d_0	initial diameter of a round bar
d_f	diameter of the fracture surface of a round bar
f_0	initial porosity
f_F	void volume fraction at the onset of fracture
f_N	potential void volume fraction that can be nucleated
f_c	void volume fraction at the onset of coalescence
f_y	yield stress
f_u	ultimate stress
q_1, q_2	material parameters introduced in GTN model
t_0	initial thickness of a specimen
t_{f1}	the largest thickness of the fracture surface of a specimen
t_{f2}	the smallest thickness of the fracture surface of a specimen
ε	logarithmic strain
ε_N, s_N	statistical void nucleation parameters
ε_{eq}	equivalent plastic strain
ε_{nom}	nominal (engineering) strain
ε_p	plastic strain
ε_q	the logarithmic strain at the end of the yield plateau of coupon tests
ε_s	critical strain parameter in the SMGTN model
σ	true stress
σ_1, σ_2 and σ_3	the first, second and third principal stress
σ_{nom}	nominal stress measured by the uniaxial coupon tests
σ_y	matrix yield stress
τ_{max}	the maximum shear stress
$(\tau_{max})_c$	critical value of the maximum shear stress

However, the above simulations have two main disadvantages that must be overcome to achieve accurate fracture simulations for tubular joints. Firstly, the fracture models employed to predict and simulate the fracture of tubular joints were not well calibrated due to the absence of coupon tests with different stress states. Considering that fractures normally occur at the welding area, fracture models should be calibrated for both the tubular members and the welds. Secondly, both tensile and shear fracture modes may be observed during the fracture of tubular joints as a result of the complex joint geometry. Therefore, the reliability of the employed fracture models in predicting fractures under different stress states must be examined.

This paper presents a full-range test on a hot-rolled seamless square hollow section (SHS) X-joint, which is carefully conducted to provide a benchmark for future fracture simulation of tubular joints, and a reliable method for simulation of fracture and post-fracture behaviour of tubular joints. The tested X-joint was loaded under axial load until fracture occurred at the welds causing the totally failure of the joint. For the SHS members and the weld used in the joint, there were three types of specimens, i.e., the traditional tensile specimen, the notched specimen and the shear specimen. The fracture model employed in this study, i.e., the GTN model, was thus calibrated based on a proposed simplified calibration procedure. FE simulation results showed that the original GTN model was capable of predicting the fracture initiation, which is driven by tensile stress states, but failed to predict the fracture propagation under shear stress states. Hence, a shear modification on the GTN model was proposed to accommodate the shear fracture mode. The modified GTN model (SMGTN) was utilised in a new FE simulation, and the results demonstrated a better accuracy of the SMGTN over the original GTN model, especially in the post-fracture stage.

2. Experimental study on a tubular SHS X-joint

2.1. Specimen details

The tested SHS X-joint had two 480-mm-long braces connected perpendicularly at the centre of a 600-mm-long chord, as shown in Fig. 1. The chord section had a 200-mm outer width, and a measured average thickness of 8.1 mm. The brace section had a 120-mm outer width, and a measured average thickness of 6.1 mm. Both sections had an outside corner radius of 20 mm. All tubular members were made from seamless Q345B steel tubes. Fillet welds made from even-matching weld metal, i.e., E50 type weld, were adopted to connect the braces to the chord, and the measured throat thickness averaged 7.2 mm.

2.2. Test setup

Fig. 2 shows the test setup. The test was conducted on a vertical plane within a self-equilibrating steel reaction frame. The chord member was set free at both ends. One of the two braces was fixed to and supported by the reaction frame, while the other brace was connected with a servo-controlled hydraulic actuator fixed to the reaction frame. The connection between actuator and brace became effectively a pinned end, because the in-plan rotational degrees of freedom were released at the connection.

The actuator applied monotonically increasing tension load on the brace. The loading process was load-controlled at first, with a loading rate of 25 kN/min. After the tension on the brace reached 400 kN, a deformation-controlled loading protocol was adopted with a loading rate of 0.5 mm/min until the test was terminated.

2.3. Instrumentation

The test setup incorporated six linear variable displacement transducers (LVDTs). As shown in Fig. 3, transducers D1 and D2 were mounted parallel to the brace axis on the south and north sides of the joint, respectively, to measure U_1, which is the averaged deformation along the brace axis in the joint area. D1 and D2 started 120 mm (equal to the diameter of the braces) above the top surface of the joint and ended 120 mm below the bottom surface of the joint.

Transducers D3 and D4 were mounted perpendicular to the south and north lateral surfaces of the chord, respectively. D3 and D4 started at the central point of the south and north lateral surface of the chord, respectively, and ended 1500 mm away from their start points. Transducers D5 and D6 were mounted along the axis of the braces. D5 and D6 started at the central point of the south and north lateral surface

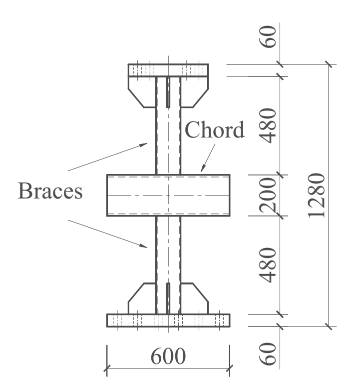

Fig. 1. Geometry of specimen (unit: mm).